HHS Public Access

Author manuscript

J Biomech. Author manuscript; available in PMC 2018 July 26.

Published in final edited form as:

J Biomech. 2017 July 26; 60: 124–133. doi:10.1016/j.jbiomech.2017.06.013.

Arterial Wall Remodeling under Sustained Axial Twisting in Rats

Guo-Liang Wang[1,3], **Li-Yi Wang**[1], **Shao-Xiong Yang**[2], **Ping Zhang**[1], **Xiao-Hu Chen**[1], **Qing-Ping Yao**[1], **Xiao-Bo Gong**[1,2], **Ying-Xin Qi**[1], **Zong-Lai Jiang**[1,*], and **Hai-Chao Han**[1,3,*]

[1]Institute of Mechanobiology and Medical Engineering, School of Life Sciences and Biotechnology, Shanghai Jiao Tong University, Shanghai 200240, China

[2]Department of Engineering Mechanics, Shanghai Jiao Tong University, Shanghai 200240, China

[3]Department of Mechanical Engineering, University of Texas at San Antonio, San Antonio, TX 78249, USA

Abstract

Blood vessels often experience torsion along their axes and it is essential to understand their biological responses and wall remodeling under torsion. To this end, a rat model was developed to investigate the arterial wall remodeling under sustained axial twisting *in vivo*. Rat carotid arteries were twisted at 180 degrees along the longitudinal axis through a surgical procedure and maintained for different durations up to 4 weeks. The wall remodeling in these twisted arteries was examined using histology, immunohistochemistry and fluorescent microscopy. Our data showed that arteries remodeled under twisting in a time-dependent manner during the 4 weeks post-surgery. Cell proliferation, MMP-2 and MMP-9 expressions, medial wall thickness and lumen diameter increased while collagen to elastin ratio decreased. While the size and number of internal elastic lamina fenestrae increased with elongated shapes, the endothelial cells elongated and aligned towards the blood flow direction gradually. These results demonstrated that sustained axial twisting results in artery remodeling *in vivo*. The rat carotid artery twisting model is an effective *in vivo* model for studying arterial wall remodeling under long-term torsion. These results enrich our understanding of vascular biology and arterial wall remodeling under mechanical stresses.

Keywords

Artery twist; Torsion; Shear stress; Wall remodeling; Rat; Endothelial cell; Cell proliferation; Internal elastic lamina, Fenestrae, Extracellular matrix; Matrix metalloproteinase

[*]**Please address correspondence to:** Dr. Hai-Chao Han, hchan@utsa.edu; Dr. Zong-Lai Jiang, zljiang@sjtu.edu.cn.

Conflict of interest

The authors have no conflict of interest.

INTRODUCTION

Arteries *in vivo* are subjected to complex mechanical loads due to lumen blood flow, pressure, surrounding tissue tethering, and body movement. It is well documented that alterations in lumen flow, pressure and axial stretch lead to arterial wall remodeling (Ku 1997; Han et al. 2003; Lawrence and Gooch 2009; Lee et al. 2010; Chiu and Chien 2011; Hayman et al. 2012; Bell et al. 2016). The remodeling is characterized by structural and cellular changes such as increases in lumen size and wall thickness, extracellular matrix (ECM) deposition, cell proliferation, and matrix metalloproteinase (MMP) expressions, as well as the adaptation of endothelial cell (EC) shape and alignment (Langille 1996; Ku 1997; Nerem et al. 1998; Han et al. 2003; Gleason et al. 2004; Lee et al. 2008; Kim et al. 2009; Chiu and Chien 2011).

Arteries also often experience axial twisting due to body movement or surgical procedures (Barton and Margolis 1975; Pao et al. 1992; Han et al. 1998; Norris et al. 2000; Dobrin et al. 2001; Ding et al. 2002; Selvaggi et al. 2004). Mobile arteries within the torso and lower extremities such as the iliac, superficial femoral, and femoropopliteal are subjected to torsion with hip and knee flexion (Cheng et al. 2006; Choi et al. 2009; Klein et al. 2009). Sustained twisting occurs in arteries in vivo due to pathological changes or vascular surgery procedures (Salgarello et al. 2001; Kalish et al. 2003; Topalan et al. 2003; Wong et al. 2007). It also occurs in perforator-based propeller flap procedures for skin grafting in which a skin island, still connected to its' perforating artery and vein, is elevated and rotated like a helicopter propeller up to 180° using the perforating vessels as a pivot point (Jakubietz et al. 2007; Chang et al. 2009). However, little is known about arterial wall remodeling induced by axial twisting though it is known that torsion alters the arterial wall stress (Humphrey 2002; Garcia et al. 2013).

Severe twisting of arteries and veins can affect their patency, impair endothelium function and delay wound healing in the anastomosis area, and lead to distal ischemia (Barton and Margolis 1975; Endean et al. 1989; Izquierdo et al. 1998; Topalan et al. 2003; Selvaggi et al. 2004; Garcia et al. 2017). These changes can cause increased risks for thrombosis and organ dysfunction (Endean et al. 1989; Bilgin et al. 2003; Selvaggi et al. 2004; Chesnutt and Han 2011). It has been reported that cervical artery is extremely vulnerable to torsion injury that can lead to dissection and stroke (Norris et al. 2000). In order to better understand the artery functional change and augment vascular healing, it is essential to understand the mechanical behavior and biological responses as well as the adaptive remodeling of arteries under sustained axial twisting (Deng et al. 1994; Lu et al. 2003; Van Epps and Vorp 2008; Garcia et al. 2013; Han et al. 2013).

Previously, we developed an *ex vivo* porcine carotid artery twisting model (Wang et al. 2015). It was shown that arterial wall remodels under axial twisting as demonstrated by elevated cell proliferation and MMP expression, changes in EC shape and orientation, as well as internal elastic lamina (IEL) fenestrae shape in 3 days under axial twisting. However, there has been no long-term study reported partially due to the limited duration of arteries in the organ culture model. Therefore, it is necessary to develop an animal model to investigate the long-term arterial remodeling under axial twisting.

Accordingly, the goal of this study was to investigate arterial wall remodeling under sustained axial twisting. A rat carotid artery twisting model was developed and the resulting arterial wall remodeling was investigated for up to 4 weeks.

MATERIALS AND METHODS

Animal

Male Sprague-Dawley rats, 9–10 weeks old, body weight 280–300 g, purchased from the SLAC Laboratory Animal Center were used in this study. The rats were randomly divided into experimental (twisting) and control (no-twisting) groups. The animal care and experimental protocols were approved by the Animal Management Committee in SJTU and implemented following the Animal Management Rules of China (Documentation 55, 2001, Ministry of Health, China).

Surgical Procedure

Rats in the experimental groups were anesthetized with 1–2% isoflurane in oxygen, intubated, placed on a standard rodent ventilator, and prepared following the protocol detailed in our previous report (Zhang et al. 2014). Using sterile techniques, a midline cervical incision was made and the left carotid artery (~20–25 mm) was exposed and dissected from surrounding tissues. A segment of 5 mm in length located at about 5 mm away from the common carotid bifurcation was marked for twisting. After blood flow was stopped with hemostatic clamps, a rigid semi-circular tubular sheath (1.3 mm in diameter, 5 mm in length, BD Vialon™ biomaterial developed by BD Medical) was placed underneath the arterial segment to facilitate twisting (Fig. 1a). Two pairs of surgical sutures (silk 10–0, Jinhuan Medical Products Co., China) were sewn to the surface (adventitia) of the artery at the two sides at the proximal and distal ends of the segment, respectively (Fig. 1b). The two sutures at the proximal end were first tied to the sheath to attach the artery segment to the sheath (Fig. 1c). Two sutures at the distal end were then pulled to swap locations to rotate the distal end of the artery segment by 180° and were sewn to the scaffold accordingly after the rotation (Fig. 1d). The rigid sheath served as scaffold to maintain the twist in the arterial segment. Then, the hemostatic clamps were released to restore blood flow and the incision was closed. The 180° twist angle was used since it is an angle that occurs in vessels in skin flaps (Jakubietz et al. 2007; Chang et al. 2009). It is also convenient for operation and no twist buckling (lumen collapse) occurred at this twist angle.

In the control groups, sham operation was done similarly only without rotating the distal end of the artery segment.

After surgery, the animals were under close care and kept warm until fully awake and then sent back to the vivarium and maintained with standard diet and tap water.

Experimental Group Design and Tissue Harvesting

All rats of experimental groups were divided into 5 sets which includes a total of 16 groups for examining different indexes of arterial wall remodeling (Table 1). Specifically, cell proliferation, extracellular matrix contents, IEL fenestrae morphology, EC morphology, and

MMP activities were examined separated in different sets of animals as described below. The use of different sets of animals for different measurements was to overcome the constraint of small tissue size of each artery segment which was not sufficient for all measurement. Each set of rats was divided into 3 groups to survive for 3 time points, 3 d, 1 wk and 4 wk, to examine the temporal changes. An additional (16^{th}) group was designated for silver staining at day 0, in which fresh arterial segments were immediately processed for silver staining when the twisting is applied. Sixteen control groups (sham operation) were assigned to match each of the 16 groups in the 5 experimental sets.

All the arteries remained patent and the twist remained evident until the day of harvesting. On the designated date (3 d, 1 wk or 4 wk after surgery), animals were anesthetized with isoflurane, the left carotid arteries were exposed, harvested and separated from the sheath, and then animals were sacrificed.

Histology and Photometric Measurement

For histology, rat systemic vasculature was perfused with 4% paraformaldehyde (Sigma-Aldrich) at a physiological pressure of 100 mmHg for 2 hours (Guo et al. 2008). The left carotid arteries were then carefully removed, washed in sterile phosphate buffer saline (PBS), and kept in 4% paraformaldehyde overnight. Then, the specimens were dehydrated in graded alcohol and frozen section (5 μm) were cut using a microtome (Leica CM3050S, Germany). The sections were stained with Haematoxylin-Eosin (H&E) staining, Van Gieson staining, and Verhoeff staining, for general, collagen, and elastin contents, respectively, and examined with light microscope. Due to extensive scar post-surgery, we excluded the measurement on adventitia. The lumen and outer diameters of the medial layer, as well as the intima-media wall thickness were measured. The wall thickness to lumen diameter ratio was then determined (Han and Ku 2001; Wang et al. 2015). The collagen and elastin contents were quantified as the ratio of the area occupied by collagen and elastin fibers divided by the total area of the media, respectively, and the collagen to elastin (C/E) ratio was calculated as an index of arterial (medial wall) stiffness (Jones et al. 2009; Zhang et al. 2013).

IEL Remodeling

The IEL was examined following the protocol described in detail previously (Guo et al. 2008; Yao et al. 2009). Briefly, after perfusion fixation as described above, artery segments were cut open longitudinally, laid with lumen side up, covered with mounting medium, and observed *en face* using a confocal microscope (Olympus, FV1000) utilizing the autofluorescence characteristic of the IEL. For each sample, five view fields were photographed under a 40× oil immersion objective. Later, the aspect ratio and size of individual fenestrae as well as the overall number, density, and area percentage of the fenestrae were quantified using Image-Pro Plus.

Cell Proliferation Labeling and Quantification

Twenty-four hours prior to harvesting, the rats were treated with a single intraperitoneal injection of Bromodeoxyuridine (BrdU, 50 mg/kg bodyweight, Sigma-Aldrich) to label new proliferating cells (Xiao et al. 2014; Qi et al. 2016). After the animals were sacrificed, the

left carotid arteries were harvested, cut into 5 μm frozen slides as described above and processed for BrdU staining (Wang et al. 2015). Cell proliferation was quantified by the ratio of the proliferating cells to counterstained all vascular cells (Xiao et al. 2014; Wang et al. 2015).

Characterization of EC Shape and Alignment

The EC shape and alignment were examined following the protocol described previously (Lee et al. 2008; Wang et al. 2015). Briefly, the arterial segments were perfused with silver nitrate to impregnate ECs and fixed under a pressure 100 mmHg for 2 hours. The arterial segments were then harvested and cut open longitudinally, placed on glass slides with the lumen side up, and examined via *en face* light microscopy.

For each sample, 5 view fields were photographed under bright field. Using these photos, EC contours were tracked manually using Image-Pro Plus and the morphological parameters such as area, major and minor axis lengths were measured and the cell shape index was calculated as described previously (Wang et al. 2015). For each artery sample, about 500 ECs were measured and the mean value was calculated to represent the value for each artery.

Immunoblotting

The arterial segments were washed three times with sterile PBS, weighed, minced on ice, ground with tissue lyser (Scientz, China), centrifuged, homogenized with 2x loading buffer, and stored at −80°C. The expression of MMP-2 and MMP-9 were examined using standard Western blot analysis described previously (Wang et al. 2015). The separated protein extracts were detected with the following primary antibodies: Anti-MMP-2 (1:500, Millipore), Anti-MMP-9 (1:300, Millipore) and anti-GAPDH (1:1000, Sigma). The photometric intensities of the protein bands were quantified using ImageJ.

Determination of Strain and Stress

The stress and strain in the twisted arteries were estimated based on the axi-symmetric cylindrical vessel model (Garcia et al. 2013). The shear strain and principal strain direction were determined using the methods as previously described (Wang et al. 2015; Garcia et al. 2017). Briefly, arteries were modeled as circular cylinders under an axial force (N), lumen pressure (P_i), and torque (T). The inner radius, outer radius and length of vessel are designated by (R_i, R_e, L) at the no-load configuration and (r_i, r_e l) at the loaded configuration, respectively. The deformation of the artery is defined by an axial stretch ratio (λ_o) and twists angle (ϕ). Using the cylindrical coordinates, the deformation gradient matrix (F) under torsion is (Fung 1993; Humphrey 2002; Garcia et al. 2013).

$$\mathbf{F}=\begin{bmatrix} \lambda_r & 0 & 0 \\ 0 & \lambda_\theta & r\gamma \\ 0 & 0 & \lambda_o \end{bmatrix} = \begin{bmatrix} \frac{\partial r}{\partial R} & 0 & 0 \\ 0 & \frac{r}{R} & r\gamma \\ 0 & 0 & \lambda_o \end{bmatrix} \quad (1)$$

where γ is the twist per unit unloaded length ($\gamma = \phi/L$), λ_r, λ_θ, and λ_0 are the radial, circumferential, and axial stretch ratios in the artery, respectively. Accordingly, the strains are given by $E = (F^T F - I)$.

To determine the principal direction (angle α) in the vessel wall surface plane (θ-z), the eigenvector of the sub-matrix below was determined.

$$E_{2D} = \frac{1}{2}\begin{bmatrix} \left(\frac{r}{R}\right)^2 - 1 & \frac{r^2\gamma}{R} \\ \frac{r^2\gamma}{R} & (r\gamma)^2 + (\lambda_0)^2 - 1 \end{bmatrix} \quad (2)$$

To estimate the wall stress in the arterial wall, we used the exponential Fung strain energy function (w) with the incompressibility assumption (Fung 1993; Humphrey 2002; Garcia et al. 2013):

$$w = \frac{1}{2} b_0 e^Q + K\left[(1+2E_r)(1+2E_\theta)(1+2E_z) - 4(1+2E_r)E_{\theta z}^2 - 1\right]$$

$$Q = b_1 E_\theta^2 + b_2 E_z^2 + b_3 E_r^2 + 2b_4 E_\theta E_z + 2b_5 E_z E_r + 2b_6 E_r E_\theta + 2b_7 E_{\theta z}^2 \quad (3)$$

Where b_0, b_1 to b_7 are dimensional material constants, and K is a Lagrange multiplier. The stress is determined by:

$$\boldsymbol{\sigma} = \mathbf{2F} \cdot \frac{\partial \mathrm{W}}{\partial \mathbf{E}} \cdot \mathbf{F}^{\mathrm{T}} \quad (4)$$

Based on the equilibrium for the cylindrical vessels, the lumen pressure, axial force, and axial torque can be expressed as (Humphrey 2002; Lee et al. 2012; Garcia et al. 2013):

$$P_i = \int_{r_i}^{r_e} (\sigma_{\theta\theta} - \sigma_{rr}) \frac{dr}{r} \quad (5)$$

$$N = \pi \int_{r_i}^{r_e} (2\sigma_{zz} - \sigma_{rr} - \sigma_{\theta\theta}) r dr + \pi r_i^2 P_i \quad (6)$$

$$T = 2\pi \int_{r_i}^{r_e} \sigma_{\theta z} r^2 dr \quad (7)$$

The stress distribution in the arteries were determined using these equations.

Due to the limited tissue sample size, we were not able to perform inflation and twist testing to determine the material constants for rat arteries. So the material constants for porcine carotid arteries (Garcia et al. 2013) were used in model simulations to illustrate the stress distribution. The *in vivo* outer diameter and segment length were measured using the photos taken during the surgical procedure. The outer and inner diameters at a pressure of 100 mmHg were measured from the frozen slides. These dimensions were used in the model analysis.

Statistical Analysis

Data were presented as mean ± *SD*. Statistical significance between means was determined using Student's *t*-test for two group comparisons or ANOVA for multiple-group comparisons. A value of $p < 0.05$ was considered statistically significant, and $p < 0.01$ was considered highly significant.

RESULTS

Stress and Strain Distribution

Using the dimensions measured *in vivo* and *in vitro*, the shear strain in the circumferential-axial plane in the twisted arteries were estimated to be 20.1 ± 1.7° and the principal strain directions were determined to be 9.3 ± 3.5° from the axial (flow) direction. The *in vivo* axial stretch ratio was measured to be 1.35 ± 0.12. Further stress analysis showed that the axial twisting had no effect on the axial and radial stresses, slightly reduced circumferential stress, but significantly increased the shear stress $\sigma_{\theta z}$ in the circumferential-axial plane (Fig. 2). The maximum increase happened at lumen wall.

Wall Thickness and Lumen Diameter

The lumen diameter, medial wall thickness and the medial wall thickness to lumen diameter ratio showed no statistical difference between the twisting group and corresponding control group, respectively, at the 3 days and 1 week post surgery (Fig. 3). However, they all increased significantly in the twisting group at 4 weeks ($p < 0.05$), indicating that sustained twisting induced significant arterial wall structural remodeling.

Collagen and Elastin contents

The collagen and elastin contents showed no difference between twisting and control groups, respectively, at 3 days and 1 week. However, the collagen content decreased significantly at 4 weeks ($p < 0.01$) while elastin content remained unchanged. Accordingly, C/E ratio decreased significantly as well (Fig. 4).

IEL fenestrae

The mean area and total area of fenestrae showed a consistent significant increase from 3 days ($p < 0.01$) to 4 weeks ($p < 0.05$) but the shape showed notable elongation only at 3 days ($p < 0.01$). The numbers of the fenestrae per unit area showed no change at 3 days, yet considerable increases in 1 week ($p < 0.01$) and 4 weeks ($p < 0.05$, Fig. 5).

Cell Proliferation

New proliferating cells significantly increased in the twisted arteries in both intima and media layers at 3 days and 1 week compared to the corresponding controls (Fig. 6, $p < 0.01$). Interestingly, cell proliferation rate returned to the same as in the controls in 4 weeks.

Adaptation of EC Shape and Alignment

ECs in the twisted arteries adapted their shape and alignment over the duration of 4 weeks. When the twisting was applied initially (day 0), the EC mean orientation angle immediately changed to 12.2 ± 5.4° while their shapes and areas showed no change. After 3 days, the mean orientation angle reduced to 10.6 ± 5.9° while the shape showed significant elongation; after 1 week, the mean orientation angle further reduced to 4.2 ± 1.6°, the shape kept elongated; after 4 weeks, the orientation was 4.0 ± 3.6°, and the shape recovered to the same as the corresponding controls (Fig. 7). The strain analysis showed that axial twisting shifted the principal strain directions from the initial axial (flow) direction to an inclined angle. A comparison of EC alignment angles (Fig.8) suggested that a) the EC alignment was eventually controlled by the flow direction (which is in the axial direction), not the principal strain direction, b) the ECs reorientation adapted in similar patterns in the current rat carotid artery model and the previous porcine carotid artery organ culture model (Wang et al. 2015).

MMP-2, MMP-9 expression

Western blotting results showed that MMP-2 ($p < 0.05$) and MMP-9 ($p < 0.01$) expressions were significantly increased in the twisting group compared to the control group only at 3 days, and returned to the same as the corresponding controls after 1 week (Fig. 9).

Discussion

In this study, a rat model to twist carotid arteries *in vivo* was developed and the wall remodeling under sustained twisting was investigated. Our results demonstrated that the axial twisting increased cell proliferation, IEL fenestrae area, MMP-2 and MMP-9 expressions in the early stage. It is followed by increased arterial medial wall thickness and the medial wall thickness to lumen diameter ratio while decreasing the collagen to elastin ratio in the media, which is a novel finding of the study. The orientation of ECs in the twisted arteries adapted towards blood flow direction while their shape became elongated. Model simulations showed that axial twisting significantly increased the wall shear stress in the circumferential-axial plane.

The current results from the *in vivo* model are consistent with our previous observations in porcine arteries under twisting using an *ex vivo* organ culture model (Wang et al. 2015). The early increases in cell proliferation, IEL fenestrae area and MMP-2 and MMP-9 expression as well as the changes in EC morphology and alignment are very similar. The novelty of this study lies in the development and use of the *in vivo* model which allows us to examine the adaptation over a longer period of time. A new finding is that arteries adapt to axial twisting by increasing lumen diameter, medial wall thickness and the medial wall thickness to lumen diameter ratio in 4 weeks.

Interestingly, we found that medial wall thickness increased at 4 weeks after twisting even though the collagen content in the media decreased. Since smooth muscle cells are the dominating component in the media, the significant increase in cell proliferation could be the reason for the relative increase in medial wall thickness.

Due to constraint of limited artery tissue available for testing, we were not able to measure the arterial wall stiffness directly. The C/E ratio was calculated as an indicator of arterial stiffness, since it has been shown to relate to arterial distensibility and stiffness (Jones et al. 2009; Sindram et al. 2011; Wang et al. 2016). Our results showed that the C/E ratio decreased significantly, indicating that the arterial medial wall stiffness could be reduced by sustained axial twisting. One limitation of the model analysis was the assumption of axi-symmetry based on initial normal arterial wall structure. It is possible that with the tissue remodeling under axial twisting, arteries wall could become non-axisymmetric (Liu et al. 2015). The possible non-symmetric mechanical behavior and wall remodeling under axial twisting needs further study (Han et al. 2013).

Numerous studies have demonstrated that MMPs play a crucial role in maintaining vascular homeostasis and is a precursor of ECM remodeling (Galis and Khatri 2002; Yabluchanskiy et al. 2013). Our results showed that MMP-2 and MMP-9 expressions increased significantly at 3 days after axial twisting, followed by ECM changes in 4 weeks. While the features of increased cell proliferation, and MMP expression under axial twisting are similar to the features of the wall remodeling due to elevated pressure, axial stretch and pulse pressure (Han and Ku 2001; Jackson et al. 2002; Han et al. 2003; Gleason et al. 2007; Hayman et al. 2012), other features, such as the decrease in collagen content under axial twisting, are different from wall remodeling under elevated pressure and axial stretch, which demonstrated increased collagen contents (Langille 1996; Jackson et al. 2002; Kim et al. 2009). In addition, previous studies showed EC would adapt to flow or axial stretch in a few days (Flaherty et al. 1972; McCue et al. 2006; Lee et al. 2008; Chiu and Chien 2011; Michaelis 2014). Similarly, IEL fenestrae morphology were known to change with elevated pulse pressure and cyclic stretch (Jackson et al. 2002; Yao et al. 2009). Our current results showed EC and IEL fenestrae in the twisted arteries also adapted their shape and alignment. These results broaden our understanding of stress-induced wall remodeling by defining the effects of torsional wall shear stress.

The remodeling of arteries under axial twisting may affect vascular function and the possible pathological effects remain to be defined. Further studies are needed to examine the possible link between axial twist and vascular diseases.

CONCLUSION

Using a newly developed rat model, this study showed that sustained axial twisting of arteries stimulates cell proliferation and ECM remodeling and affects EC morphology. These results enrich our understanding of vascular biology and mechanical behavior and demonstrated that axial twisting can stimulate *in vivo* artery remodeling.

Acknowledgments

This work was supported by National Natural Science Foundation of China through grants, Nos.11229202, 11232010, and by the National Institutes of Health through grant R01HL095852.

References

Barton JW, Margolis MT. Rotational obstructions of the vertebral artery at the atlantoaxial joint. Neuroradiology. 1975; 9(3):117–20. [PubMed: 1161138]

Bell ED, Donato AJ, Monson KL. Cerebrovascular dysfunction following subfailure axial stretch. J Mech Behav Biomed Mater. 2016; 65:627–633. [PubMed: 27736719]

Bilgin SS, Topalan M, Ip WY, Chow SP. Effect of torsion on microvenous anastomotic patency in a rat model and early thrombolytic phenomenon. Microsurgery. 2003; 23(4):381–386. [PubMed: 12942531]

Chang CH, Lim SY, Pyon JK, Bang SI, Oh KS, Mun GH. The Influence of Pedicle Length on the Viability of Twisted Perforator Flaps in Rats. Journal of Reconstructive Microsurgery. 2009; 25(9): 533–538. [PubMed: 19676024]

Cheng CP, Wilson NM, Hallett RL, Herfkens RJ, Taylor CA. In vivo MR angiographic quantification of axial and twisting deformations of the superficial femoral artery resulting from maximum hip and knee flexion. Journal of Vascular and Interventional Radiology. 2006; 17(6):979–987. [PubMed: 16778231]

Chesnutt JK, Han HC. Tortuosity triggers platelet activation and thrombus formation in microvessels. J Biomech Eng. 2011; 133(12):121004. [PubMed: 22206421]

Chiu JJ, Chien S. Effects of Disturbed Flow on Vascular Endothelium: Pathophysiological Basis and Clinical Perspectives. Physiological Reviews. 2011; 91(1):327–387. [PubMed: 21248169]

Choi G, Shin LK, Taylor CA, Cheng CP. In Vivo Deformation of the Human Abdominal Aorta and Common Iliac Arteries With Hip and Knee Flexion: Implications for the Design of Stent-Grafts. Journal of Endovascular Therapy. 2009; 16(5):531–538. [PubMed: 19842734]

Deng SX, Tomioka J, Debes JC, Fung YC. New experiments on shear modulus of elasticity of arteries. Am J Physiol. 1994; 266(1 Pt 2):H1–10. [PubMed: 8304490]

Ding Z, Zhu H, Friedman MH. Coronary artery dynamics in vivo. Ann Biomed Eng. 2002; 30(4):419–29. [PubMed: 12085995]

Dobrin PB, Hodgett D, Canfield T, Mrkvicka R. Mechanical determinants of graft kinking. Ann Vasc Surg. 2001; 15(3):343–9. [PubMed: 11414086]

Endean ED, DeJong S, Dobrin PB. Effect of twist on flow and patency of vein grafts. J Vasc Surg. 1989; 9(5):651–5. [PubMed: 2724454]

Flaherty JT, Pierce JE, Ferrans VJ, Patel DJ, Tucker WK, Fry DL. Endothelial nuclear patterns in the canine arterial tree with particular reference to hemodynamic events. Circ Res. 1972; 30(1):23–33. [PubMed: 5007525]

Fung, YC. Biomechanics: Mechanical Properties of Living Tissues. New YorK: Springer Verlag; 1993.

Galis ZS, Khatri JJ. Matrix metalloproteinases in vascular remodeling and atherogenesis: the good, the bad, and the ugly. Circ Res. 2002; 90(3):251–62. [PubMed: 11861412]

Garcia JR, Lamm SD, Han HC. Twist buckling behavior of arteries. Biomech Model Mechanobiol. 2013; 12(5):915–927. [PubMed: 23160845]

Garcia JR, Sanyal A, Fatemifar F, Mottahedi M, Han HC. Twist buckling of veins under torsional loading. J Biomech. 2017; 58:123–130. [PubMed: 28526174]

Gleason RL, Taber LA, Humphrey JD. A 2-D model of flow-induced alterations in the geometry, structure, and properties of carotid arteries. J Biomech Eng. 2004; 126(3):371–81. [PubMed: 15341175]

Gleason RL, Wilson E, Humphrey JD. Biaxial biomechanical adaptations of mouse carotid arteries cultured at altered axial extension. J Biomech. 2007; 40(4):766–76. [PubMed: 16750537]

Guo ZY, Yan ZQ, Bai L, Zhang ML, Jiang ZL. Flow shear stress affects macromolecular accumulation through modulation of internal elastic lamina fenestrae. Clinical Biomechanics. 2008; 23:S104–S111. [PubMed: 17923177]

Han HC, Chesnutt JKW, Garcia JR, Liu Q, Wen Q. Artery Buckling: New Phenotypes, Models, and Applications. Ann Biomed Eng. 2013; 41(7):1399–1410. [PubMed: 23192265]

Han HC, Ku DN. Contractile responses in arteries subjected to hypertensive pressure in seven-day organ culture. Ann Biomed Eng. 2001; 29(6):467–75. [PubMed: 11459340]

Han HC, Ku DN, Vito RP. Arterial wall adaptation under elevated longitudinal stretch in organ culture. Ann Biomed Eng. 2003; 31(4):403–11. [PubMed: 12723681]

Han HC, Zhao L, Huang M, Hou LS, Huang YT, Kuang ZB. Postsurgical changes of the opening angle of canine autogenous vein graft. J Biomech Eng. 1998; 120(2):211–6. [PubMed: 10412382]

Hayman DM, Xiao Y, Yao Q, Jiang Z, Lindsey ML, Han HC. Alterations in Pulse Pressure Affect Artery Function. Cell Mol Bioeng. 2012; 5(4):474–487. [PubMed: 23243477]

Humphrey, JD. Cardiovascular solid mechanics: cells, tissues, and organs. New York: Springer; 2002.

Izquierdo R, Dobrin PB, Fu K, Park F, Galante G. The effect of twist on microvascular anastomotic patency and angiographic luminal dimensions. J Surg Res. 1998; 78(1):60–3. [PubMed: 9733619]

Jackson ZS, Gotlieb AI, Langille BL. Wall tissue remodeling regulates longitudinal tension in arteries. Circ Res. 2002; 90(8):918–25. [PubMed: 11988494]

Jakubietz RG, Jakubietz MG, Gruenert JG, Kloss DF. The 180-degree perforator-based, propeller flap for soft tissue coverage of the distal, lower extremity - A new method to achieve reliable coverage of the distal lower extremity with a local, fasciocutaneous perforator flap. Annals of Plastic Surgery. 2007; 59(6):667–671. [PubMed: 18046150]

Jones JA, Beck C, Barbour JR, Zavadzkas JA, Mukherjee R, Spinale FG, Ikonomidis JS. Alterations in aortic cellular constituents during thoracic aortic aneurysm development: myofibroblast-mediated vascular remodeling. Am J Pathol. 2009; 175(4):1746–56. [PubMed: 19729479]

Kalish RB, Hunter T, Sharma G, Baergen RN. Clinical significance of the umbilical cord twist. Am J Obstet Gynecol. 2003; 189(3):736–9. [PubMed: 14526304]

Kim YS, Galis ZS, Rachev A, Han HC, Vito RP. Matrix metalloproteinase-2 and -9 are associated with high stresses predicted using a nonlinear heterogeneous model of arteries. J Biomech Eng. 2009; 131(1):011009. [PubMed: 19045925]

Klein AJ, Chen SJ, Messenger JC, Hansgen AR, Plomondon ME, Carroll JD, Casserly IP. Quantitative assessment of the conformational change in the femoropopliteal artery with leg movement. Catheter Cardiovasc Interv. 2009; 74(5):787–98. [PubMed: 19521998]

Ku DN. Blood flow in arteries. Ann Rev Fluid Mech. 1997; 29(1):399–434.

Langille BL. Arterial remodeling: relation to hemodynamics. Can J Physiol Pharmacol. 1996; 74(7): 834–41. [PubMed: 8946070]

Lawrence AR, Gooch KJ. Transmural pressure and axial loading interactively regulate arterial remodeling ex vivo. Am J Physiol Heart Circ Physiol. 2009; 297(1):H475–H484. [PubMed: 19465545]

Lee AY, Han B, Lamm SD, Fierro CA, Han HC. Effects of elastin degradation and surrounding matrix support on artery stability. Am J Physiol Heart Circ Physiol. 2012; 302(4):H873–84. [PubMed: 22159998]

Lee YU, Hayman D, Sprague EA, Han HC. Effects of Axial Stretch on Cell Proliferation and Intimal Thickness in Arteries in Organ Culture. Cell Mol Bioeng. 2010; 3(3):286–295. [PubMed: 21116478]

Lee YU, Drury-Stewart D, Vito RP, Han HC. Morphologic adaptation of arterial endothelial cells to longitudinal stretch in organ culture. J Biomech. 2008; 41(15):3274–7. [PubMed: 18922530]

Liu, Q., Baek, S., Han, HC. Annual meeting of Biomedical Engineering Society. Tampa, Florida: 2015. Growth and Remodeling of Artery under Twisting. 2015

Lu X, Yang J, Zhao JB, Gregersen H, Kassab GS. Shear modulus of porcine coronary artery: contributions of media and adventitia. Am J Physiol Heart Circ Physiol. 2003; 285(5):H1966–75. [PubMed: 14561679]

McCue S, Dajnowiec D, Xu F, Zhang M, Jackson MR, Langille BL. Shear stress regulates forward and reverse planar cell polarity of vascular endothelium in vivo and in vitro. Circulation Research. 2006; 98(7):939–946. [PubMed: 16527990]

Michaelis UR. Mechanisms of endothelial cell migration. Cell Mol Life Sci. 2014; 71(21):4131–48. [PubMed: 25038776]

Nerem RM, Alexander RW, Chappell DC, Medford RM, Varner SE, Taylor WR. The study of the influence of flow on vascular endothelial biology. Am J Med Sci. 1998; 316(3):169–75. [PubMed: 9749558]

Norris JW, Beletsky V, Nadareishvili ZG. Sudden neck movement and cervical artery dissection. The Canadian Stroke Consortium. CMAJ. 2000; 163(1):38–40. [PubMed: 10920729]

Pao YC, Lu JT, Ritman EL. Bending and Twisting of an In Vivo Coronary Artery at a Bifurcation. J Biomech. 1992; 25(3):287–295. [PubMed: 1564062]

Qi YX, Yao QP, Huang K, Shi Q, Zhang P, Wang GL, Han Y, Bao H, Wang L, Li HP, Shen BR, Wang Y, Chien S, Jiang ZL. Nuclear envelope proteins modulate proliferation of vascular smooth muscle cells during cyclic stretch application. Proc Natl Acad Sci U S A. 2016

Salgarello M, Lahoud P, Selvaggi G, Gentileschi S, Sturla M, Farallo E. The effect of twisting on microanastomotic patency of arteries and veins in a rat model. Ann Plast Surg. 2001; 47(6):643–6. [PubMed: 11756835]

Selvaggi G, Salgarello M, Farallo E, Anicic S, Formaggia L. Effect of torsion on microvenous anastomotic patency in rat model and early thrombolytic phenomenon. Microsurgery. 2004; 24(5): 416–7. [PubMed: 15378589]

Sindram D, Martin K, Meadows JP, Prabhu AS, Heath JJ, McKillop IH, Iannitti DA. Collagen-elastin ratio predicts burst pressure of arterial seals created using a bipolar vessel sealing device in a porcine model. Surg Endosc. 2011; 25(8):2604–12. [PubMed: 21404086]

Topalan M, Bilgin SS, Ip WY, Chow SP. Effect of torsion on microarterial anastomosis patency. Microsurgery. 2003; 23(1):56–9. [PubMed: 12616520]

Van Epps JS, Vorp DA. A new three-dimensional exponential material model of the coronary arterial wall to include shear stress due to torsion. Journal of Biomechanical Engineering-Transactions of the Asme. 2008; 130(5)

Wang GL, Xiao Y, Voorhees A, Qi YX, Jiang ZL, Han HC. Artery Remodeling Under Axial Twist in Three Days Organ Culture. Ann Biomed Eng. 2015; 43(8):1738–47. [PubMed: 25503524]

Wang Y, Zeinali-Davarani S, Zhang Y. Arterial mechanics considering the structural and mechanical contributions of ECM constituents. J Biomech. 2016; 49(12):2358–65. [PubMed: 26947034]

Wong CH, Cui F, Tan BK, Liu Z, Lee HP, Lu C, Foo CL, Song C. Nonlinear finite element simulations to elucidate the determinants of perforator patency in propeller flaps. Ann Plast Surg. 2007; 59(6): 672–8. [PubMed: 18046151]

Xiao Y, Hayman D, Khalafvand SS, Lindsey ML, Han HC. Artery Buckling Stimulates Cell Proliferation and NF-kappaB Signaling. Am J Physiol Heart Circ Physiol. 2014

Yabluchanskiy A, Ma Y, Iyer RP, Hall ME, Lindsey ML. Matrix metalloproteinase-9: Many shades of function in cardiovascular disease. Physiology (Bethesda). 2013; 28(6):391–403. [PubMed: 24186934]

Yao Q, Hayman DM, Dai Q, Lindsey ML, Han HC. Alterations of pulse pressure stimulate arterial wall matrix remodeling. J Biomech Eng. 2009; 131(10):101011. [PubMed: 19831481]

Zhang J, Liu Q, Han HC. An In Vivo Rat Model of Artery Buckling for Studying Wall Remodeling. Ann Biomed Eng. 2014; 42(8):1658–67. [PubMed: 24793586]

Zhang XY, Shen BR, Zhang YC, Wan XJ, Yao QP, Wu GL, Wang JY, Chen SG, Yan ZQ, Jiang ZL. Induction of thoracic aortic remodeling by endothelial-specific deletion of microRNA-21 in mice. Plos One. 2013; 8(3):e59002. [PubMed: 23527070]

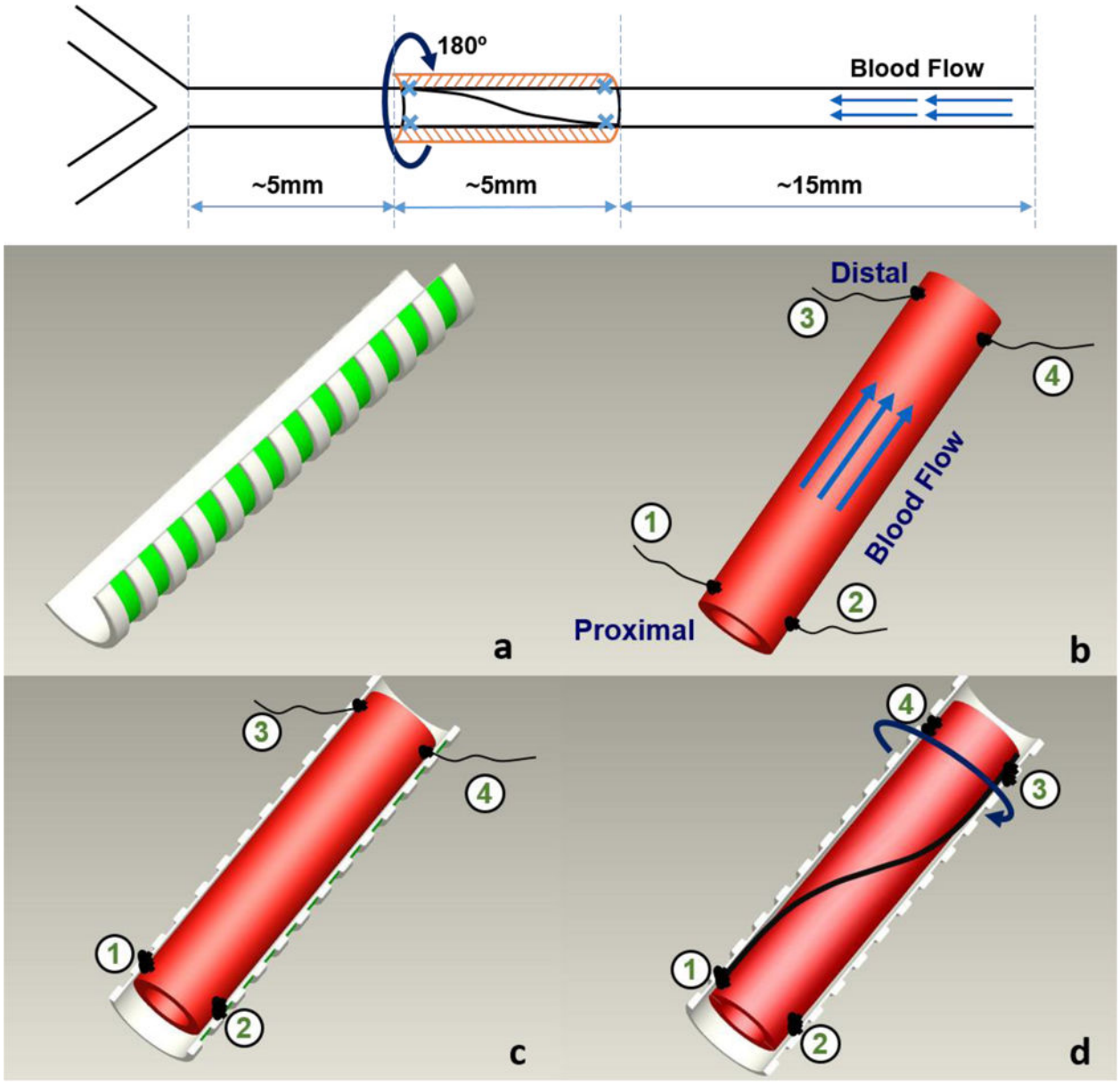

Figure 1. Schematics illustrating the twisting of rat carotid artery *in vivo*

Top: location and dimension of the twisting segment. Bottom: surgical procedure: a) rigid semi-circular tubular sheath to support twisting; b) artery segment selected with 4 sutures attached to adventitia (2 at two sides of the vessel at the proximal and distal ends, respectively; c) Two sutures at the proximal end were sewn onto the sheath. d) The two sutures at the distal end were first swapped position to rotate (twist) the vessel 180° along its axis, and then sewn onto the sheath to hold the twist in the artery segment.

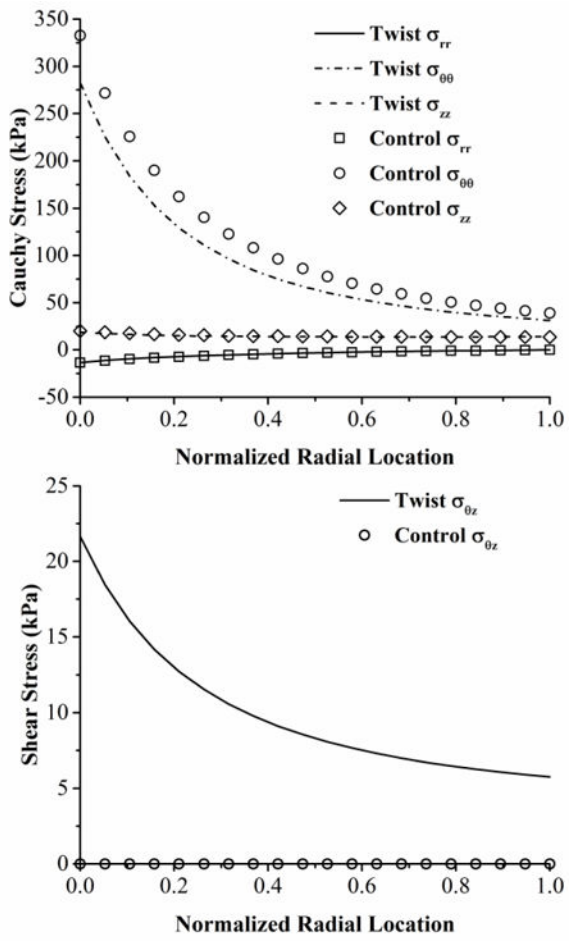

Figure 2. Stress distribution in arterial wall under axial twisting

Distribution of normal stresses (top panel) and shear stress (bottom panel) across the wall thickness in an artery under an axial twist angle of 180 degree and a physiological lumen pressure of 100 mmHg and an axial stretch ratio of 1.35. Parametric studies showed that the trend holds true independent of the material constants used.

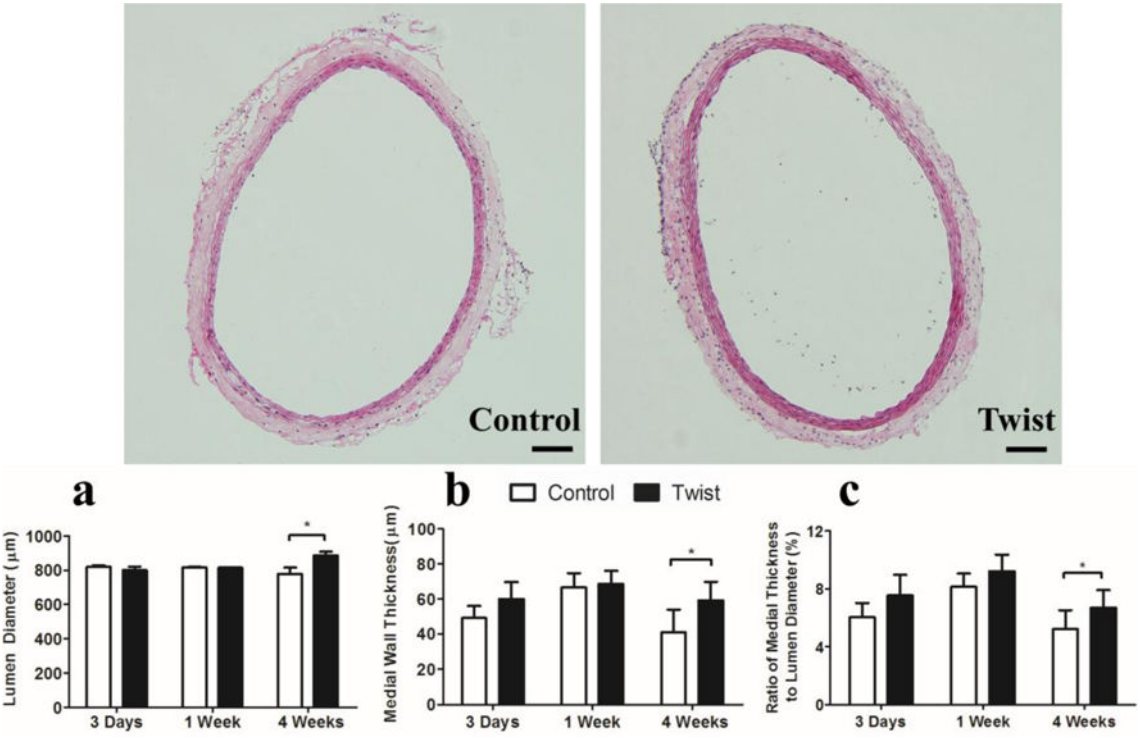

Figure 3. Twist increases the medial wall thickness to lumen diameter ratio

Photographs: Representative cross-sectional images of control and twisted arteries. H&E stain, Scale bar represent 100 μm. *Bargraphs*: Comparisons of arterial lumen diameter (a), medial wall thickness (b) and medial wall thickness to lumen diameter ratio (c) of control and twisted arteries. Values are mean ± *SD, n* = 6, * $p < 0.05$ twisted *vs.* controls.

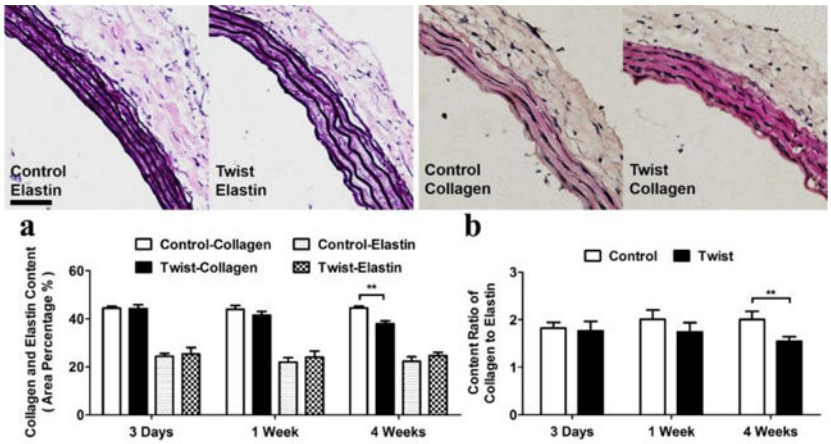

Figure 4. Twist decreases medial wall collagen to elastin ratio

Photographs: Representative images of arterial cross section with elastin (Verhoeff) and collagen (Van Gieson) staining of the control and twisted arteries. Scale bar represent 100 μm. *Bargraphs*: Left: comparison of elastin and collagen contents (mean ± *SD, n=6*) in the control and twisted arteries. Right: comparison of collagen to elastin ratio (mean ± *SD, n=6*) in the control and twisted arteries. ** $p < 0.01$ *vs.* controls.

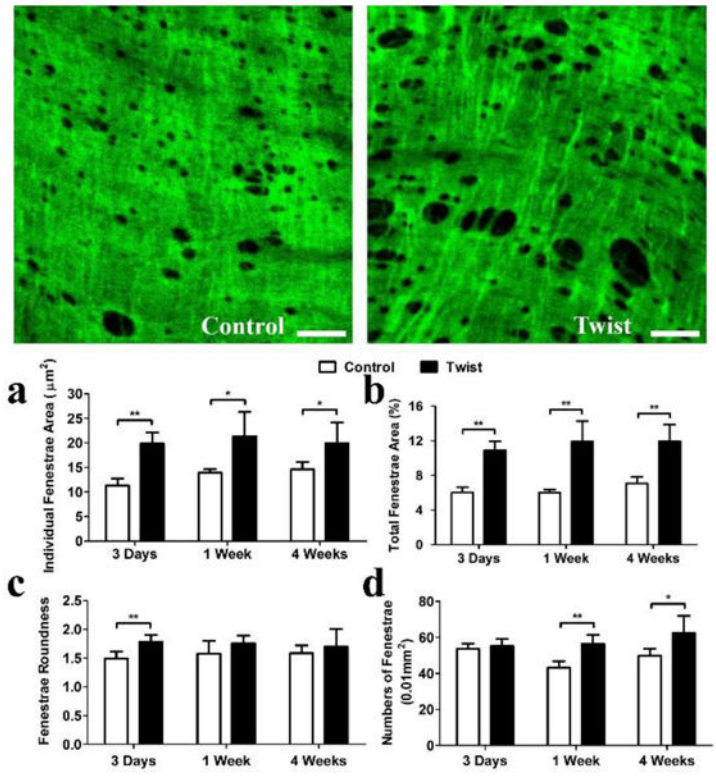

Figure 5. IEL fenestrae shape and area changes over time

Photographs: Representative en face confocal images of IEL fenestrae of arteries from control and twist group at 1 week. Scale bar represent 20μm. *Bargraphs*: Comparison of a) mean fenestrae area; b) total fenestrae area; c) fenestrae roundness, and d) fenestrae numbers, between the control and twisted arteries at 3 time points. * $p < 0.05$ *vs*. controls, ** $p < 0.01$ *vs*. controls. $n = 5$.

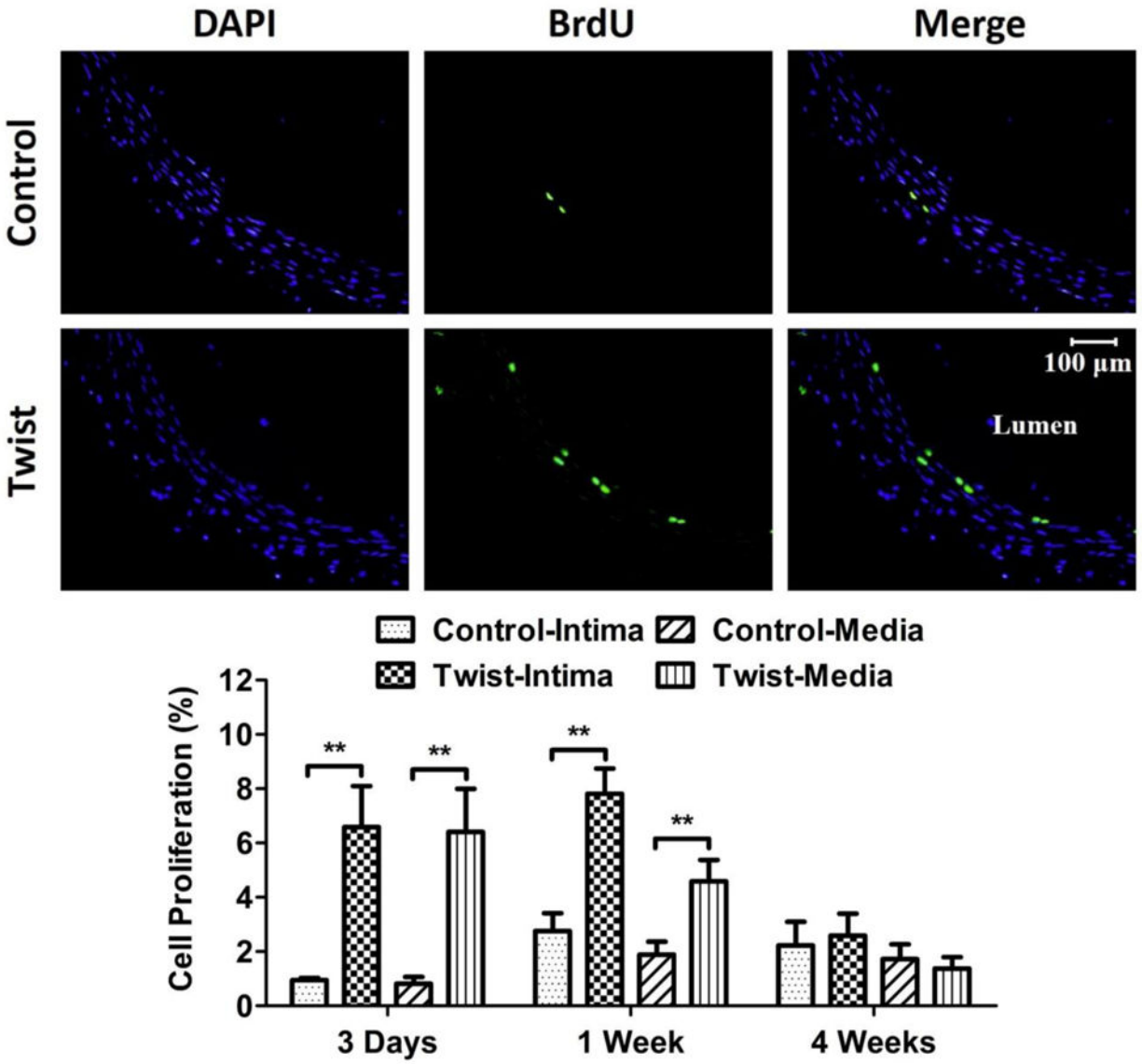

Figure 6. Twist induces cell proliferation in the arterial wall

Photographs: Representative cross-sectional images of DAPI counter-staining and BrdU staining of the control and twisted arteries. *Bargraphs*: Comparison of cell proliferation ratio (mean ± *SD, n=6*) in the intima and media of arteries from the control and twist groups. ** $p < 0.01$ *vs.* controls.

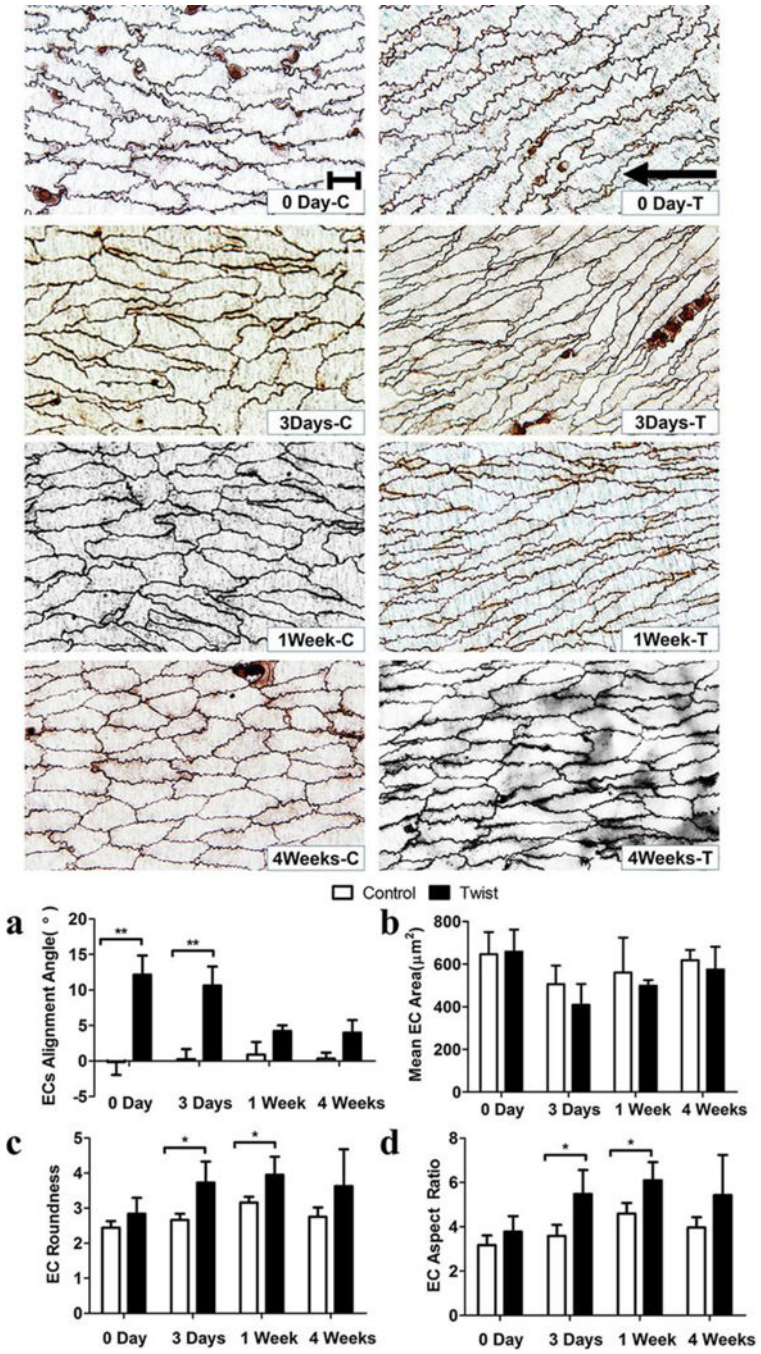

Figure 7. Twist induces EC shape and orientation changes

Top: Micrographs from en face light microscopy illustrating the contours of endothelial cell visualized by silver staining. Scale bar represent 20 μm. "C" and "T" in the labels represent control and twisted arteries. Arrow indicates the flow direction. *Bargraphs*: Comparisons of (a) EC alignment angle, (b) EC area (size), (c) EC roundness, and (d) EC aspect ratio in the control and twisting groups. Values are mean ± *SD*, $n = 5$, * $p < 0.05$ *vs.* controls, ** $p < 0.01$ *vs.* controls.

Time	0 d	3 d	1 w	4 w	Principal Strain (θ-z)
Organ Culture					
No Twist	0.1°	0.2°			0°
Twist	15.6°	7.5°			4.6°
Rat Model					
No Twist	0.1°	0.2°	0.9°	0.3°	0°
Twist	12.2°	10.6°	4.2°	4.0°	9.3°

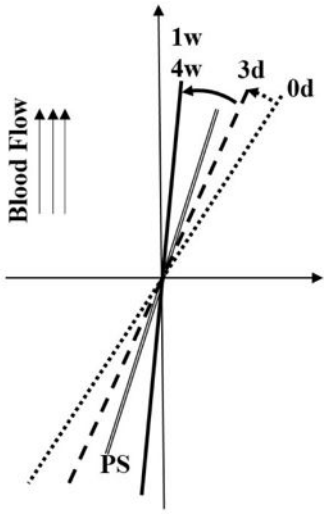

Figure 8. Comparison of EC orientation *and* principal strain direction

Table: comparison of the actual alignment angle values at different time points and with data from previous organ culture study (Wang et al., 2015). *Figure*: Illustration of EC orientation in twisted arteries at 0 day (dotted line), 3d, (dash line), 1wk & 4wks (solid line) compared to the direction of the principal strain (PS, double solid line). Angles were proportionally enlarged for better visualization.

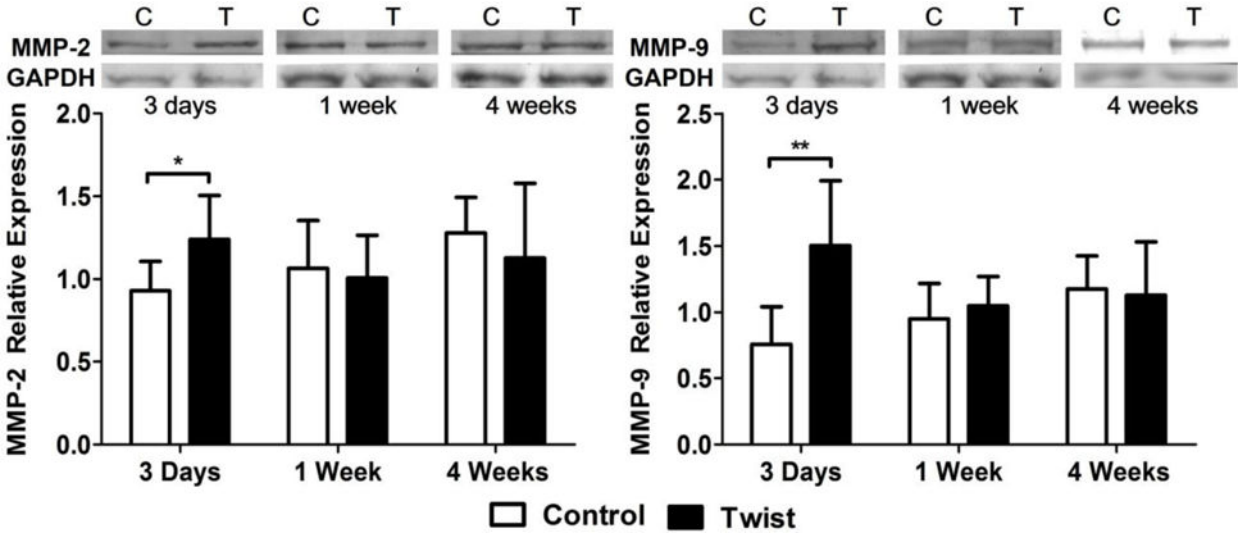

Figure 9. MMP-2 and MMP-9 expression increases in twisted arteries

Top: Representative western blotting results showing the levels of MMP-2, MMP-9 and GAPDH in the control and twisting groups. Bargraphs: Comparison of the relative intensities of MMP-2 (Left) and MMP-9 (Right) of the control and twisting groups. Values were normalized with housekeeping gene GAPDH. * $p < 0.05$ *vs.* controls, ** $p < 0.01$ *vs.* control. $n = 7$.

Table 1

Experimental design: summary of measurements in 5 experiment sets and groups in each set for different time points with sample size in each group.

Set	Measurement	Group Sample Size*			
		0 Day	3 Days	1 Week	4 Weeks
I	H&E (Wall thickness) Verhoeff (Elastin) Van Gieson (Collagen)	—	6	6	6
II	BrdU (Cell Proliferation)	—	6	6	6
III	Confocal (IEL fenestrae) Confocal (SMC Nuclei)	—	5	5	5
IV	Silver Stain (EC Morphology)	5	5	5	5
V	Western Blotting (MMP)	—	7	7	7

*Same sample size in each control group (sham operation) is the same as the corresponding experimental group.